RSC Advances

PAPER

View Article Online
View Journal | View Issue

Amphiphilic block copolymer micelles with fluorescence as nano-carriers for doxorubicin delivery

Cite this: *RSC Adv.*, 2014, **4**, 9684

Jiucun Chen[ab] and Mingzhu Liu*[a]

Received 26th November 2013
Accepted 21st January 2014

DOI: 10.1039/c3ra47026a

www.rsc.org/advances

Well-defined and nontoxic core–shell polymeric micelles, containing fluorescence units, were employed for efficient drug delivery of doxorubicin (DOX). The self-assembled structures were generated from triblock copolymers of poly(ε-caprolactone)-*block*-poly(glycidyl methacrylate)-*block*-poly(poly(ethylene glycol)methyl ether methacrylate) (PCL-*b*-PGMA-*b*-P(PEGMA)) with fluorescence units. Various experiments like structural characterization, fluorescence properties, cell viability studies, encapsulation studies, measuring cytotoxicity against fibroblasts and bladder cancer cells are performed on these polymeric micelles. All of these results demonstrate that these self-assembled micelles may be promising carriers for intravesical delivery of DOX for bladder cancer therapy.

1 Introduction

Currently, polymeric micelles as promising nanosized antitumor drug carriers are being extensively studied.[1–5] Polymeric micelles offer many unique advantages, such as passive accumulation in tumors, prolonged circulation time in blood and the enhanced uptake by tumors.[6] In particular, micelles formed from block copolymers consisting of poly(ε-caprolactone) (PCL) and poly(ethylene glycol)methyl ether methacrylate (PEGMA) have drawn considerable interest.[7–12] The PEGMA with excellent biocompatibility forms the hydrophilic corona in the micelles, thereby reducing nonspecific adhesion of micelle surfaces to blood components. PCL, as the most commonly used hydrophobic polyesters, has several particular properties, such as biocompatibility and biodegradability. Thus, PCL, serving as hydrophobic core in the micelles, can be used to load water-insoluble drugs.

The self-assembly of amphiphilic block copolymers usually requires that copolymers have well-defined structures and narrow polydispersities. Remarkable advancements in controlled radical polymerization (CRP) techniques including reversible addition-fragmentation chain transfer (RAFT)[13–15] polymerization now allow the precise construction of sophisticated architectures appropriate for use as delivery vehicles for diagnostics and therapeutic agents in the rapidly expanding area of nanomedicine.[16] Despite the versatility of CRP techniques, it is still a challenge to find feasible means to introduce functional groups onto polymer chains. These functional polymers, for example, fluorescent groups labeled polymers, biofunctionalized polymers and drug containing polymers, can find wide applications in chemistry, materials science and biomedical science fields.[17–19] As an efficient coupling reaction, the Cu(I)-catalyzed azide-alkyne cycloaddition (CuAAC), *i.e.* "click reaction", as termed by Sharpless and coworkers,[20] has gained increasing attention because of its excellent functional group tolerance, high specificity and nearly quantitative yields under mild experimental conditions.[21] Therefore, click chemistry is particularly important in chemical synthesis in which high conversion of functional groups is desired. Combining CRP with click chemistry is an efficient way to prepare functional polymeric materials.[22–26]

Bladder cancer is the second most common genitourinary malignancy and ranks ninth in worldwide cancer incidence. It is also the most expensive disease to treat from diagnosis to death (US data), due to the long-term survival associated with non muscle-invasive disease combined with life-long surveillance.[27] Therefore, it represents an important public health problem. However, few studies have reported the use of core–shell polymeric micelles as drug delivery vehicles for bladder cancer therapy. In this article, novel and well-defined amphiphilic poly(ε-caprolactone)-*block*-poly(glycidyl methacrylate)-*block*-poly(poly(ethylene glycol)methyl ether methacrylate) (PCL-*b*-PGMA-*b*-P(PEGMA)) with fluorescence units was synthesized by combination of ring-opening polymerization (ROP), RAFT and click chemistry. The polymeric micelles were obtained by self-assembly of the triblock copolymer prepared *via* RAFT polymerization. Incorporation of a block with fluorescence unit as a pendant group between the shell and core-forming blocks displays different fluorescent profiles at the interface between

[a]*State Key Laboratory of Applied Organic Chemistry, Key Laboratory of Nonferrous Metal Chemistry and Resources Utilization of Gansu Province and Department of Chemistry, Lanzhou University, Lanzhou 730000, P. R. China. E-mail: mzliu@lzu.edu.cn; Fax: +86-931-8912582; Tel: +86-931-8912387*

[b]*Institute for Clean Energy & Advanced Materials, Southwest University, Chongqing, 400715, P. R. China. E-mail: chenjc@swu.edu.cn*

the hydrophobic core and the hydrophilic shell. Moreover, loading and *in vitro* release of DOX, as well as anti-tumor activity of DOX-loaded polymeric micelles were investigated.

2 Experimental section

2.1 Materials

Poly(ethylene glycol)methyl ether methacrylate (PEGMA, Sigma-Aldrich, M_n = 475 g mol^{-1}, M_w/M_n = 1.03) and glycidyl methacrylate (GMA, Sigma-Aldrich) were passed through a basic alumina column and stored at −20 °C prior to use. 2,2′-Azobisisobutyronitrile (AIBN, Sigma-Aldrich, 97%) was recrystallized with methanol. Tetrahydrofuran (THF), doxorubicin hydrochloride (DOX), 4-cyano-4-[(dodecylsulfanylthiocarbonyl)sulfanyl]pentanol (CDP), ε-caprolactone (CL), 7-hydroxy coumarin, copper(I) bromide (CuBr), stannous octanoate ($Sn(Oct)_2$), *N*,*N*,*N*′,*N*″,*N*″-pentamethyldiethylenetriamine (PMDETA) (98%), 1,4-dioxane, Dulbecco's modified Eagle medium (DMEM), fetal bovine serum (FBS), 3-(4,5-dimethyl-2-thiazolyl)-2,5-diphenyl-2*H*-tetrazolium bromide (MTT), dimethyl sulfoxide (DMSO), and *N*,*N*-dimethylformamide (DMF) were purchased from Sigma-Aldrich Chem. Co. All other regents and solvents were purchased either from Sigma-Aldrich or Merck Chem. Co. and were used as received. The artificial urine used in the experimental work was based on that devised by Griffith *et al.*[28]

Fibroblasts (3T3) and Human bladder cancer cells (UMUC3) were purchased from American Type Culture Collection.

2.2 Characterization

The nuclear magnetic resonance (^{1}H NMR) spectra were obtained from a Bruker Avance 400 spectrometer (Bruker Bio-Spin, Switzerland) (400 MHz). The molecular mass and molecular weight distribution were measured by gel permeation chromatography (GPC) on a Hitachi L-2130 pump with a Waters 2410 refractive index detector and a Waters 2487 ultraviolet detector with the combination of Hersteller MZ-Gel SDplus 5 mm, and the THF was used as eluent at a flow rate of 1.0 mL min^{-1}. Fourier transform infrared (FTIR) spectroscopy patterns were performed on a Nicolet 670 (U.S.A.) IR spectrometer. The spectra were collected at 64 scans with a spectral resolution of 2 cm^{-1}. Transmission electron microscopy (TEM) was performed using a Tecnai G220 TEM operated at an accelerating voltage of 200 kV. The samples were prepared by dropping 10 mL of 0.1 mg mL^{-1} polymersome dispersion on the copper grid. The size of polymersomes was determined using dynamic light scattering (DLS). Measurements were carried out at 25 °C using Zetasizer Nano ZS from Malvern Instruments equipped with a 633 nm He–Ne laser using back-scattering detection. The UV-visible absorption spectra were obtained from a Shimadzu UV-3600 spectrophotometer. The fluorescence spectra were measured on a Shimadzu RF-5031 spectrophotometer at an excitation wavelength of 330 nm.

2.3 Synthesis of the PCL-CTA macro-RAFT agent

The ROP of CL was performed at a feed ratio of $[CL]_0/[CDP]_0/[Sn(Oct)_2]_0$ = 300/2/1 at 110 °C. CL (9.2 g, 80.70 mmol), CDP (0.210 g, 0.54 mmol), and $Sn(Oct)_2$ (0.111 g, 0.27 mmol) were dissolved in 9 mL of toluene, and the mixture was degassed by purging with nitrogen for 30 min. Polymerization was carried out at 110 °C for 24 h. The resulting PCL-CTA was precipitated in an excess of cold ether, filtered, and dried under vacuum for 24 h.

2.4 Synthesis of PCL-*b*-PGMA by RAFT

The linear diblock copolymer of PCL-*b*-PGMA was synthesized by the polymerization of GMA in the presence of the PCL-CTA macro-RAFT agent. A 25 mL Schlenk flask with a magnetic stir bar and a rubber septum was charged with PCL-CTA (3.5 g, 0.20 mmol), GMA (1.29 g, 10.0 mmol), AIBN (0.006 g, 0.04 mmol), and toluene (10 mL). The flask was deoxygenated by three freeze–pump–thaw cycles, and then sealed followed by immersing the flask into an oil bath preheated at 60 °C to start the polymerization. After reaction for 6 h, the mixture was then quickly cooled to room temperature with cool water. The reaction mixture was diluted with a little THF and precipitated in a large amount of ether. The polymer was obtained by filtration and dried at room temperature in vacuum to a constant weight.

2.5 Synthesis of triblock copolymers PCL-*b*-PGMA-*b*-P(PEGMA)

The triblock copolymers were synthesized *via* chain-extending RAFT polymerization of PEGMA using the previously synthesized PCL-*b*-PGMA copolymers as macromolecular chain transfer agents (Scheme 1). PCL-*b*-PGMA (1.386 g, 0.06 mmol), AIBN (2 mg, 0.012 mmol) and PEGMA (2.85 g, 6.0 mmol) were dissolved in 1,4-dioxane (10 mL) in a 25 mL round-bottom flask under stirring. This flask was capped with rubber septa. The solution was deoxygenated by purging with nitrogen gas for 30 min. Polymerization was carried out at 80 °C for 24 h and the polymer was precipitated into cold hexane. The polymer was reprecipitated three times from THF–hexane and dried under a vacuum at room temperature for 12 h.

2.6 Reaction of PCL-*b*-PGMA-*b*-P(PEGMA) with sodium azide

PCL-*b*-PGMA-*b*-P(PEGMA) (1.2 g, 0.54 mmol of epoxide groups) was dissolved in DMF (10 mL). Sodium azide (0.07 g, 1.08 mmol) and ammonium chloride (0.06 g, 1.1 mmol) were added to this solution, and the mixture was stirred at 50 °C for 24 h. The final reaction solution was diluted with DMF and purified by dialysis against water to remove any traces of salts and unreacted reactants using a membrane with molecular weight cutoff of 14 000 Da. The azide-containing polymers were collected by freeze-drying.

2.7 Synthesis of 7-propinyloxy coumarin (PC)

The synthesis procedure was carried out according to ref. 29. A mixture of 7-hydroxy coumarin (1.62 g, 10 mmol) in acetone (25 mL), K_2CO_3 (1.38 g, 10 mmol), KI (0.083 g, 0.5 mmol) and propargyl bromide (1.2 mL, 15 mmol) was added to a flask, and the mixture was stirred over night at 80 °C. Then the reaction mixture was cooled to room temperature and extracted with CH_2Cl_2 (3 × 50 mL). The combined organic extracts were washed with water (2 × 50 mL), dried over anhydrous $MgSO_4$ and evaporated to afford a crude product, which was purified

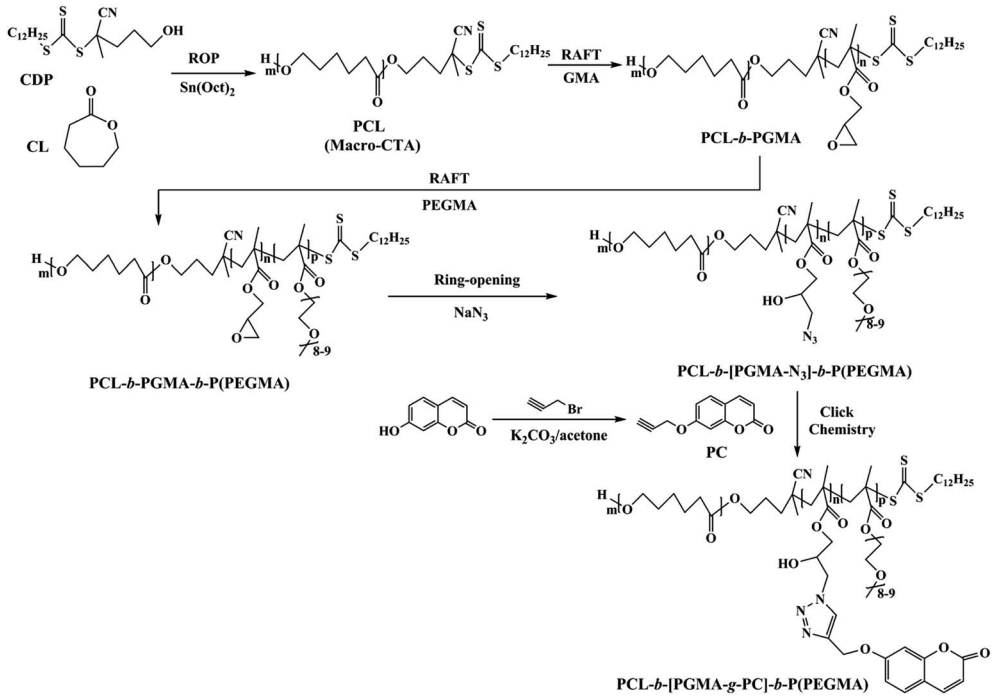

Scheme 1 Synthesis of PCL-*b*-[PGMA-*g*-PC]-*b*-P(PEGMA) conjugates by ROP, RAFT and click chemistry.

by recrystallization from anhydrous ethanol to give a white solid (71% yield).

2.8 Click grafting of PC units onto azide-containing polymeric backbones

The synthetic pathway is shown in Scheme 1. Azide-containing polymers (1.0 g, 0.017 mmol), PMDETA (83 μL, 0.40 mmol), and PC (0.16 g, 0.80 mmol) was purged with nitrogen to remove the dissolved oxygen. CuBr (57 mg, 0.40 mmol) was added under nitrogen atmosphere. Then the ampoule was flame-sealed and stirred at 25 °C in the absence of oxygen for 24 h. The reaction mixture was exposed to air, and diluted by DMF, then passed through a column of neutral alumina. The resultant polymer (PCL-*b*-[PGMA-*g*-PC]-*b*-P(PEGMA)) was precipitated into ether and hexane, respectively, filtered and dried under vacuum.

2.9 Self-assembly of triblock copolymer

PCL-*b*-[PGMA-*g*-PC]-*b*-P(PEGMA) (100 mg) was dissolved in DMF (8 mL), which is a good solvent for the hydrophobic and the hydrophilic block. Then, the solution was added dropwise using a syringe pump (3 mL h^{-1}) to water (80 mL) under high-speed stirring at room temperature. The observation of a cloudy solution indicated the formation of polymeric micelles in the mixture. After 5 h, the mixture was then dialyzed against water for 48 h using a dialysis membrane (MWCO 3500 Da) to remove DMF. The targeted final polymer concentration was 1 mg mL^{-1}.

2.10 DOX encapsulation and release studies

The encapsulation, 200 mg of PCL-*b*-[PGMA-*g*-PC]-*b*-P(PEGMA) and 20 mg of DOX, were dissolved in 8 mL of DMF separately and the two solutions were mixed in a vial and stirred for 30 min. Triethylamine (5 μL) was added and the solution was allowed for equilibration 12 h. Then the mixture was added dropwise using a syringe pump to water (170 mL) under high-speed stirring. The DOX-containing suspension was then equilibrated under stirring at 25 °C for 5 h, followed by thorough dialysis (MWCO 3500 Da) against deionized water for 2 days to remove unloaded DOX. To determine the drug loading level, a small portion of DOX-loaded micelles was withdrawn and diluted with DMF to a volume ratio of DMF–H_2O = 9/1. The amount of DOX encapsulated was quantitatively determined by a UV/vis spectrophotometer. The emission spectrum was recorded in the range 400–550 nm. The calibration curve used for drug loading characterization was established by the intensity of DOX with different concentrations in DMF–H_2O (9/1 (v/v)) solutions. Drug loading content (DLC) and drug loading efficiency (DLE) were calculated according to the following formulae:

$$\text{DLC (wt\%)} = (\text{weight of loaded drug/weight of polymer}) \times 100\%$$

$$\text{DLE (\%)} = (\text{weight of loaded drug/weight of drug in feed}) \times 100\%$$

The drug release profiles were determined by the dialysis technique. The DOX-loaded micelles dispersion (15 mL) was placed within a dialysis tube (MWCO 12 000), followed by dialysis against artificial urine (pH 6.1) at 37 °C. At prescribed time intervals, 5 mL of the external urine was withdrawn and replaced with an equivalent volume of fresh medium. The concentration of DOX was determined by the UV/vis using the pertinent calibration curve of DOX with various concentrations in artificial urine. The experimental results presented herein represent an average of at least triplicate measurements.

2.11 Cell culture

Fibroblasts (3T3) and Human bladder cancer cells (UMUC3) were maintained in DMEM with containing 10% FBS with penicillin (100 U mL^{-1}) and streptomycin (100 μg mL^{-1}). The cells were grown in a 5% CO_2 atmosphere in an incubator at 37 °C.

2.12 Cytotoxicity assay of the polymeric micelles

The relative cytotoxicity of polymeric micelles in 3T3 cell lines were quantitatively determined using MTT assay. All cell lines were seeded into 96 well plates at 1×10^4 cells per well and maintained in culture for 24 h at 37 °C in the medium. After 24 h medium was removed, cells were washed with PBS and medium containing different concentration of polymeric micelles were added to the designated wells. The whole experimental plate was incubated for 24 h or 72 h. A fresh 10 μL sample of MTT from 5 mg mL^{-1} stock solution was added to each well, followed by incubation for 4 h at 37 °C. After 4 h, medium from the wells were removed and 100 μL of DMSO were added to each well and incubated for 15 min, and the absorbance of the resulting solution was measured at 590 nm. The cell survivals were determined by comparison of optical density with untreated respective control cell cultures.

UMUC3 cells were seeded in a 96-well plate at a density of 5000 cells per well in DMEM (100 μL) containing 10% FBS and 1% penicillin and incubated at 37 °C for 24 h. The medium was then replaced with 100 μL of fresh medium containing either polymeric micelles or DOX-loaded micelles at varying micelles concentrations, and cells were incubated for 24 h or 72 h. Thereafter, 10 μL of MTT (5.0 mg mL^{-1}) was added into each well, followed by incubation at 37 °C for 4 h. After 4 h, medium from the wells were removed and 100 μL of DMSO were added to each well and incubated for 15 min, and the absorbance of the resulting solution was measured at 590 nm. The cell survivals were determined by comparison of optical density with untreated respective control cell cultures.

2.13 Intracellular release of DOX

The cellular uptake and intracellular release behaviors of DOX-loaded micelles were followed using UMUC3 cells. The cells were seeded on microscope slides in a 24-well plate (5×10^4 cells per well) using DMEM supplemented with 10% FBS for 24 h. 1 mL of either polymeric micelles or DOX-loaded micelles were added. The cells were incubated with either polymeric micelles or DOX-loaded micelles for 4 h at 37 °C in a humidified 5% CO_2-containing atmosphere. The culture media were removed and the cells were rinsed two times with PBS. The cells were fixed with 4% paraformaldehyde for 30 min. The solution was removed and the cells were rinsed three times with PBS. The images of cells were obtained using confocal laser scanning microscopy (CLSM) (Zeiss LSM 510 Meta, Germany).

3 Results and discussion

3.1 Synthesis and characterization of PCL-*b*-[PGMA-*g*-PC]-*b*-P(PEGMA)

The overall experiment is illustrated in Scheme 1. In this study, the hydroxyethyl-terminated CDP was used as initiator to synthesize the PCL-CTA. Then, PCL-*b*-PGMA-*b*-P(PEGMA) was synthesized by consecutive RAFT polymerization of GMA and PEGMA using PCL-CTA as a RAFT agent. The ring-opening reaction was applied to prepare polymers with azide groups from the GMA copolymers. Subsequently, the obtained azido-functionalized copolymer was involved in "click" chemistry with 7-propinyloxy coumarin to prepare fluorescent polymers.

The FTIR spectrum of the PCL-CTA is shown in Fig. 1a. The intensive absorption peak at 1735 cm^{-1} was assigned to the carbonyl band of PCL. Compared to the IR spectrum of PCL-CTA, it can be clearly observed the new peak at 904 cm^{-1} from the epoxide ring of PGMA. ^1H NMR spectrum of the PCL-CTA is shown in Fig. 2a. The typical signals of the methylene protons of the initiator CDP could be clearly detected at 1.27 ppm. The major resonance peaks (a–e) were attributed to PCL. The peak of the methylene protons was detected at 4.07 ppm when the peak of the protons of the terminal methylene could be discovered at 3.70 ppm which indicated that PCL was terminated by hydroxyl groups. The degrees of polymerization (DP) for the PCL could be calculated about 135 from the integration ratio between the methylene protons (2.32 ppm) in the repeat units and those (3.70 ppm) in the terminal unit based on ^1H NMR spectrum.

Fig. 2B exhibits a typical ^1H NMR spectrum of copolymer PCL-*b*-PGMA. It was observed that besides the dominant PCL signals, the new peaks i–k in the region of 2.6–4.4 ppm were attributable to the epoxy protons of the glycidyl groups of PGMA. The chemical shifts at 0.9–1.4 ppm (h) were associated with the methyl protons of the PGMA block. These results certificated that new PGMA segments were connected to PCL. The DP of PGMA blocks were obtained based on ^1H NMR spectrum. GPC analysis and $M_{n,NMR}$ values based on the ^1H NMR spectrum were shown in Table 1.

According to GPC results, the apparent molecular weight (M_n) and the polydispersity (M_w/M_n) of PCL-CTA are 17 500 and 1.26, respectively (Fig. 3). PCL-*b*-PGMA GPC trace shows that the elution peak shifts to higher molecular weight after the RAFT polymerization of GMA. The diblock copolymer elution peak is relatively symmetric and no discernible tailing at the lower

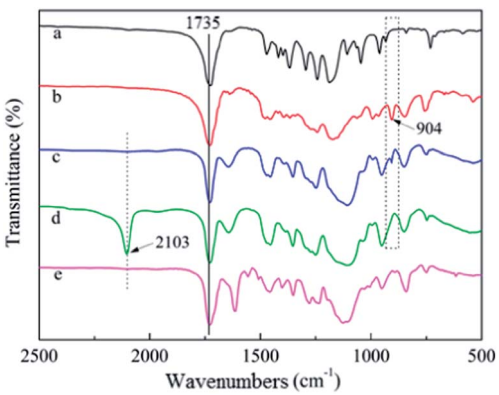

Fig. 1 FTIR spectra of (a) PCL-CTA, (b) PCL-*b*-PGMA, (c) PCL-*b*-PGMA-*b*-P(PEGMA), (d) PCL-*b*-[PGMA-N_3]-*b*-P(PEGMA), and (e) PCL-*b*-[PGMA-*g*-PC]-*b*-P(PEGMA) in $CDCl_3$.

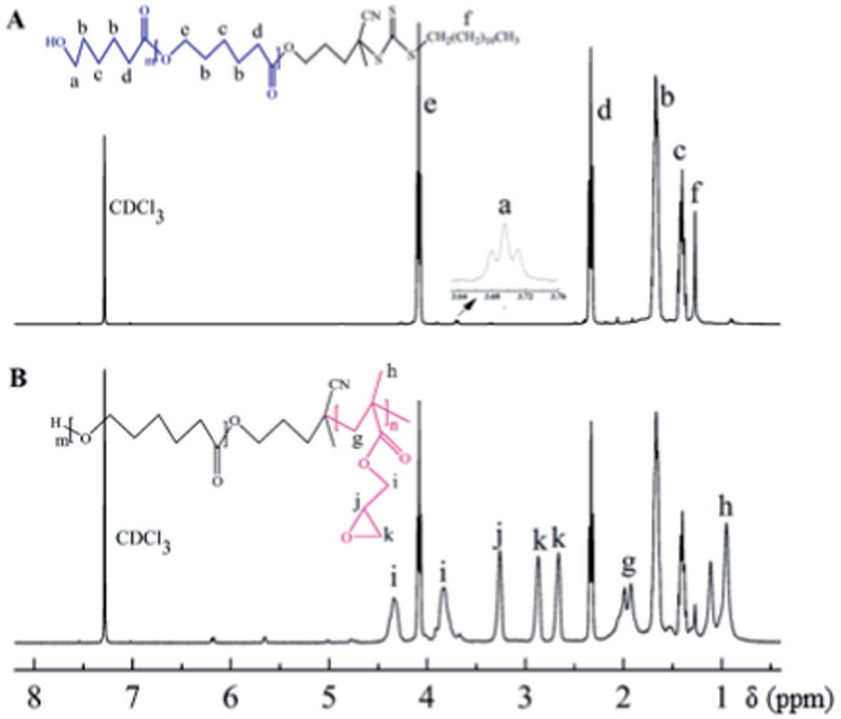

Fig. 2 ^{1}H NMR spectra of (a) PCL-CTA and (b) PCL-*b*-PGMA.

Table 1 Characterization data of copolymers synthesized by RAFT polymerization

Polymer	Conv.[a] (%)	$M_{n,th}$[b] (kDa)	DP_{NMR}[c]	$M_{n,NMR}$[c] (kDa)	$M_{n,GPC}$[d] (kDa)	PDI[d]
PCL-CTA	92	16.1	135 (PCL)	15.8	17.5	1.26
PCL-*b*-PGMA	46	20.8	24 (PGMA)	19.2	23.1	1.29
PCL-*b*-PGMA-*b*-P(PEGMA)	61	52.1	72 (P(PEGMA))	53.4	58.4	1.35
PCL-*b*-[PGMA-N_3]-*b*-P(PEGMA)	—	—	—	—	59.4	1.35
PCL-*b*-[PGMA-*g*-PC]-*b*-P(PEGMA)	—	—	—	—	64.1	1.36

[a] Conversion of monomer obtained from gravimetry. [b] Theoretical molecular weight ($M_{n,th}$) calculated by monomer conversion. [c] DP of block copolymers and $M_{n,NMR}$ were calculated on the basis of ^{1}H NMR results. [d] Number-average molecular weight ($M_{n,GPC}$) and molecular weight distribution (PDI = M_w/M_n) estimated by GPC.

molecular weight side is found, confirming a complete consumption of macro-RAFT agent.

By employing macro-CTA PCL-*b*-PGMA, PEGMA was polymerized to yield PCL-*b*-PGMA-*b*-P(PEGMA) (Scheme 1). ^{1}H NMR analysis indicates the characteristic peaks of P(PEGMA) at 4.1, 3.9–3.5, 3.4, 1.9, and 1.3–0.9 ppm attributed to CH_2O ester, CH_2O ether, CH_3O, CH_3–C, and CH_2–C backbone, respectively (Fig. 4A). The DP for the P(PEGMA) could be calculated about 72 from ^{1}H NMR. As shown in Fig. 3, GPC curves of triblock copolymer shifts to higher molecular weight direction compared with precursor polymer with slightly increased polydispersity. Synthesis of 7-propinyloxy coumarin (PC) was carried out similar to the procedure described in previous publications.[29] Resonance at 4.8 ppm was the characteristic signal of the methylene protons of propargyl group, while resonance of the alkynyl proton was observed at 2.6 ppm (Fig. 4B).

The synthesis of polymer containing azide groups for further modification is still challenging. Reaction of polymers containing epoxide groups with sodium azide at relatively moderate reaction conditions is one of the most convenient routes for preparation of polymers with azides group. After that, the epoxide groups of PCL-*b*-PGMA can be opened with sodium azide. As shown in Fig. 5A, proton signals from epoxide ring disappeared completely. Instead, newly formed resonances at 3.27, 3.35 ppm (t, $-CH_2N_3$) and enhanced resonance at 3.73–4.10 ppm demonstrated the successful transformation of epoxide to azide and hydroxyl groups. On the other hand, from the IR spectra shown in Fig. 1d, copolymer containing azide groups exhibited a typical absorbance at 2103 cm^{-1}, which is the characteristic absorbance of azide groups. By GPC analysis, the synthesis of the triblock copolymer containing azide groups precursors involved no molecular weight reduction, based on the observation of narrow symmetrical signals present at the same position as the starting PCL-*b*-PGMA-*b*-P(PEGMA) precursors (Fig. 3).

The obtained azido-functionalized copolymer was subsequently involved in "click" chemistry with 7-propinyloxy

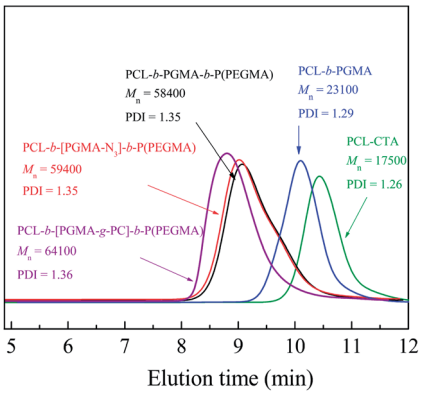

Fig. 3 GPC traces of (a) PCL-CTA, (b) PCL-*b*-PGMA, (c) PCL-*b*-PGMA-*b*-P(PEGMA), (d) PCL-*b*-[PGMA-N_3]-*b*-P(PEGMA), and (e) PCL-*b*-[PGMA-*g*-PC]-*b*-P(PEGMA).

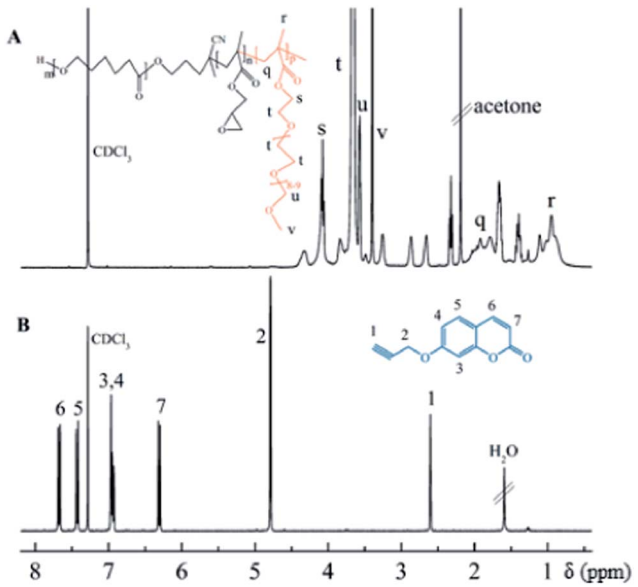

Fig. 4 ^{1}H NMR spectra of (a) PCL-*b*-PGMA-*b*-P(PEGMA) and (b) PC.

coumarin to prepare fluorescent polymers. The copper(I) and its ligands were reported to be very efficient to catalyze the 1,3-dipolar cycloaddition of organic azides with terminal alkynes. Herein, CuBr/PMDETA was used as the catalytic system, and DMF as solvent for the 1,3-dipolar cycloaddition of azido-functionalized copolymer and 7-propinyloxy coumarin. Fig. 5 shows the ^{1}H NMR spectrum recorded for PCL-*b*-[PGMA-*g*-PC]-*b*-P(PEGMA). Compared with Fig. 5A, besides the signals were assigned to the PCL and P(PEGMA), neonatal signals at 5.17 ppm due to the methylene proton neighboring the 1,2,3-triazole group, and signals at 7.80 ppm were assigned to the proton of the 1,2,3-triazole ring. The characteristic signals at around 6.70–7.10 ppm, 7.40–7.50 ppm, 7.60–7.85 ppm and 6.25–6.30 ppm were assigned to the protons of the coumarin group. Moreover, the success of the "click" reaction can also be confirmed from FTIR spectroscopy. In Fig. 1e, the IR spectra showed that the signal at 2103 cm^{-1} assigned to the

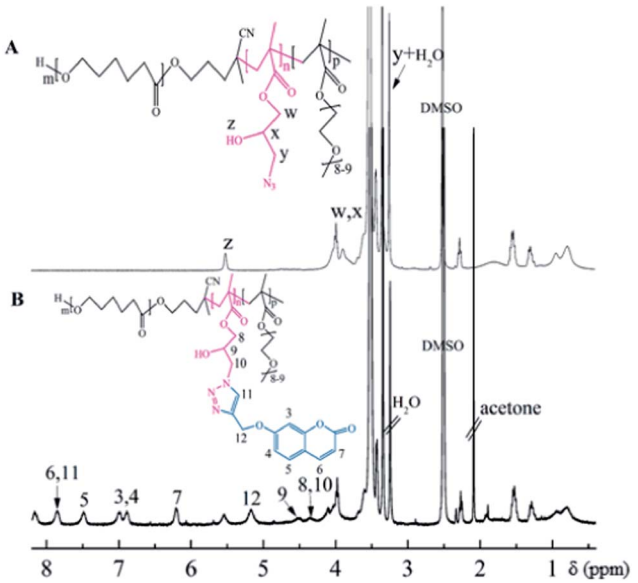

Fig. 5 ^{1}H NMR spectra of (a) PCL-*b*-[PGMA-N_3]-*b*-P(PEGMA) and (b) PCL-*b*-[PGMA-*g*-PC]-*b*-P(PEGMA).

azide group almost disappeared. Further characterization with GPC (Fig. 3) confirmed a small increase in molecular weight after coupling due to addition of the 200 g mol^{-1} PC.

3.2 Self-assembly and fluorescence properties of the triblock copolymers

The main objective of this work was to demonstrate the stability and drug reservoir capabilities of the novel amphiphilic micelles in physiological conditions and also to study their performance as a drug delivery carrier. It is well known that PCL homopolymer is hydrophobic, whereas P(PEGMA) is water-soluble at room temperature. Thus, PCL-*b*-[PGMA-*g*-PC]-*b*-P(PEGMA) micelles with core of PCL block and shell of P(PEGMA) were formed by adding polymer solution in DMF into 10 folds of water at 25 °C (Scheme 2). To confirm the micelles nature of PCL-*b*-[PGMA-*g*-PC]-*b*-P(PEGMA), the following characterization were carefully done. Light scattering measurements confirmed the presence of micelles in solution and provided an average diameter of 91 nm (Fig. 6), which implies micelles were excellent carrier for hydrophobic drug. The micelles of the amphiphilic triblock copolymers were studied by transmission electron microscopy (TEM). From Fig. 7, we can find that the micelles from the self-assembled PCL-*b*-[PGMA-*g*-PC]-*b*-P(PEGMA) in water exit excellent disperse, and the diameter of the spherical micelles vary from about 20 to 40 nm.

Fig. 8a shows the UV-vis spectra of the PCL-*b*-[PGMA-*g*-PC]-*b*-P(PEGMA), which was obtained by coupling of azide-containing polymers with 7-propinyloxy coumarin, in water at room temperature. The solution of polymeric micelles showed a characteristic UV-vis absorption peak of coumarin moiety at 320 nm. The fluorescence spectra of PCL-*b*-[PGMA-*g*-PC]-*b*-P(PEGMA) in aqueous solution are displayed in Fig. 8b. It can be observed that the triblock copolymer, obtained by coupling of

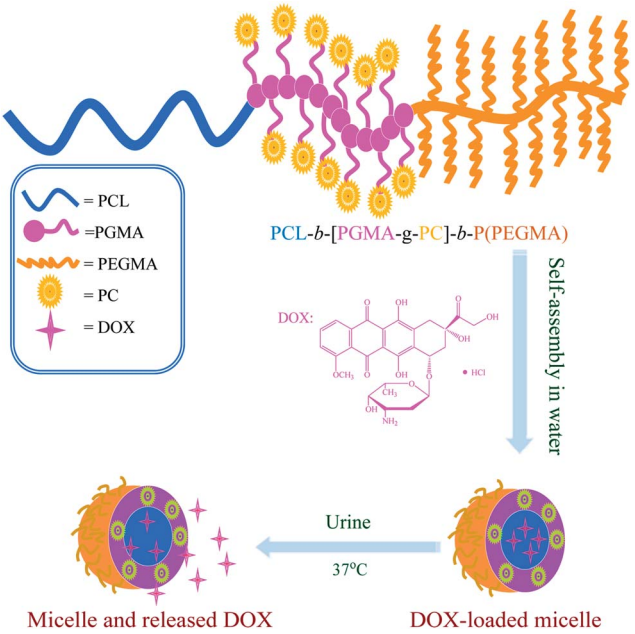

Scheme 2 Illustration of polymer micelles based on PCL-*b*-[PGMA-*g*-PC]-*b*-P(PEGMA) triblock copolymers for active loading as well as release of DOX.

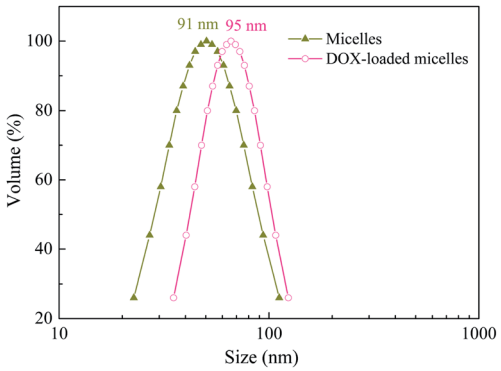

Fig. 6 Plots of hydrodynamic diameter (D_h) of micelles and DOX-loaded micelles.

azide-containing polymers with 7-propinyloxy coumarin, exhibited a strong fluorescence peak at about 390 nm.

3.3 Loading and *in vitro* release of DOX

Generally, DOX, one of the most potent anticancer drugs, is extensively used to treat different types of solid malignant tumors through interacting with DNA by interaction and inhibition of macromolecular biosynthesis. To investigate the potential of multiblock copolymer micelles based on self-assembly, DOX was selected to evaluate the drug loading and release properties. Loading of DOX into micelles was performed at a theoretical drug loading content (DLC) of 7.2 wt% and a high DOX loading efficiency of 72%. After drug loading, the size of micelles shows a slightly increased about 95 nm (Fig. 6). *In vitro* release profiles of the loaded DOX in micelles of PCL-*b*-[PGMA-*g*-PC]-*b*-P(PEGMA) copolymers were studied under a

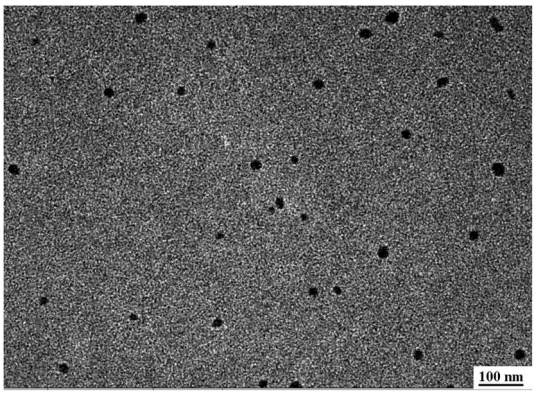

Fig. 7 TEM images of PCL-*b*-[PGMA-*g*-PC]-*b*-P(PEGMA) micelles.

simulated physiological condition at 37 °C. In artificial urine, the DOX release behaviors of the micellar carriers had the typical two-phase release profile (Fig. 9). In the first stage, about 60% DOX encapsulated in micelles released within 24 h, followed by a sustained and slow release over a prolonged time. Drug release was enhanced slightly in 72 h, wherein approximately 82% drug was released from the micelles.

3.4 Anti-tumor activity and intracellular drug release of DOX-loaded PCL-*b*-[PGMA-*g*-PC]-*b*-P(PEGMA) micelles

The cytotoxicity of PCL-*b*-[PGMA-*g*-PC]-*b*-P(PEGMA) was assessed by determining the viability of 3T3 fibroblasts after incubation in a medium containing various concentrations of pristine micelles for 24 and 72 h (Fig. 10). The MTT assay has been described as a very suitable method for the detection of biomaterial toxicity.[30] Fig. 10 demonstrates that the drug-free micelles are virtually nontoxic to 3T3 cells. The *in vitro* cytotoxicity of DOX-loaded micelles against UMUC3 cells in comparison with pristine micelles determined by MTT assay is shown in Fig. 11. Cells without any DOX treatment were used as a negative control. Compared to the control, the viability of UMUC3 cells was reduced to about 10% following 24 h incubation with 2.0 mg mL^{-1} DOX-loaded micelles. The high anti-tumor activity of DOX-loaded micelles indicates that DOX has been efficiently delivered and released into the nuclei of UMUC3 cells. While under otherwise the same conditions, pristine micelles were practically non-toxic (cell viability > 90%) up to a tested concentration of 2.0 mg mL^{-1} (Fig. 11), suggesting that pristine micelles possess good biocompatibility.

It is well known that fluorescent units with amphiphilic structures could self-assemble into vesicle/micelle-like aggregates, which are resulted from the intermolecular interaction within hydrophobic and hydrophilic moieties, respectively. Since copolymers could be designed to have different functions in the block sections, amphiphilic polymers are generally inclined to self-assemble into uniform structures. Therefore, fluorescent amphiphilic structures are usually designed as graft[31] or block[32,33] copolymers. For instance, Chang *et al.*[34] synthesized a Rhodamine B (RhB)-anchored amphiphilic poly(poly(ethylene glycol) methacrylate)-*b*-poly(glycidyl methacrylate) block copolymer (PPEGMA-*b*-PGMA/RhB), in which the

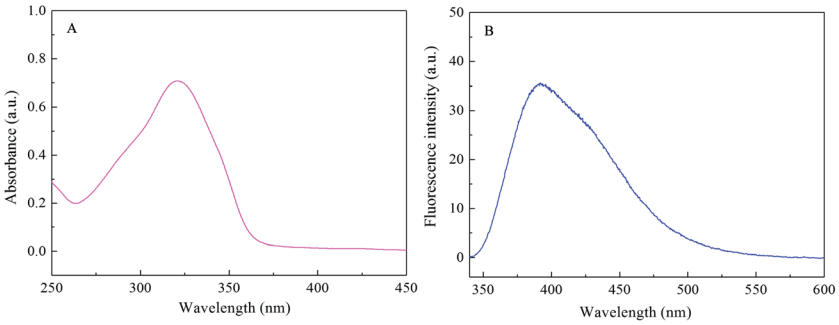

Fig. 8 (a) UV-vis spectra and (b) fluorescence spectra of PCL-*b*-[PGMA-*g*-PC]-*b*-P(PEGMA) micelles solution.

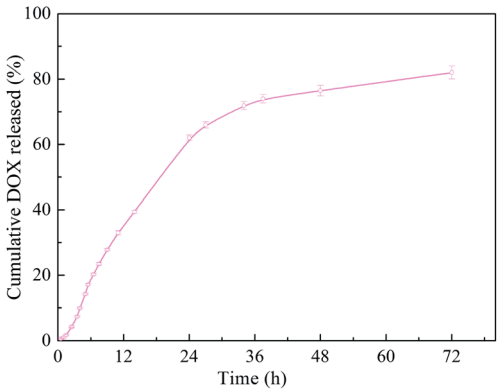

Fig. 9 Plots of release behavior of DOX-loaded micelles.

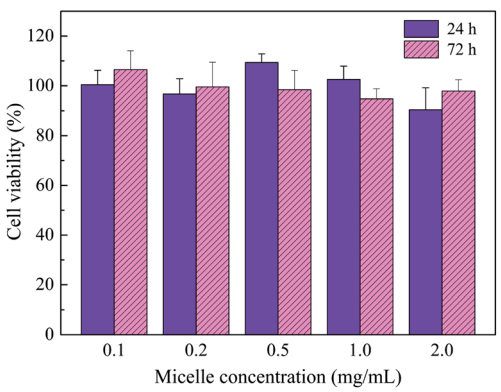

Fig. 10 Cytotoxicity of PCL-*b*-[PGMA-*g*-PC]-*b*-P(PEGMA) polymer micelles after 24 h or 72 h.

inter-molecular interaction of RhB resulted in the assembled fluorescent nanoparticles. The nanoassembly PPEGMA-*b*-PGMA/RhB was then introduced into HeLa cells and the HeLa cells exhibited good fluorescence images. Li *et al.*[31] also reported the similar results by using comb-like graft copolymer poly((*N*-vinylcarbazole)-*co*-(4-vinylbenzyl chloride))-*comb*-poly(((2-dimethylamino)ethylmethacrylate)-*co*-(acrylic acid)) to produce self-assembled hollow vesicles with multi-walls, which even exhibited good fluorescence intensity in aqueous media. In this work, cell imaging based on fluorescent polymeric micelles was subsequently investigated by CLSM. UMUC3 cells were incubated with

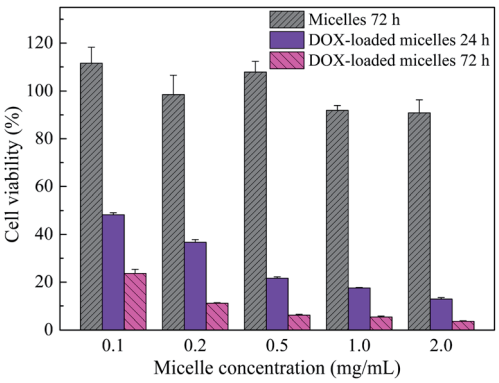

Fig. 11 Cytotoxicity of different concentration of. PCL-*b*-[PGMA-*g*-PC]-*b*-P(PEGMA) polymer micelles to UMUC3 after 24 h or 72 h.

the fluorescent polymeric micelles at the concentration of 0.5 mg mL^{-1} for 4 h. The fluorescence images of UMUC3 cells are shown in Fig. 12a. The loaded cells displayed the bright blue fluorescence corresponding to the coumarin dye, implying that the fluorescent polymeric micelles have been effectively internalized and accumulated in the cytoplasm. Furthermore, the images of UMUC3 cells treated with doxorubicin-based anticancer drug loaded PCL-*b*-[PGMA-*g*-PC]-*b*-P(PEGMA) micelles further confirmed their cellular internalization (Fig. 12b), which further exhibited their promising application for bladder cancer treatment. These results demonstrated that the fluorescent polymeric micelles have the widespread application not only in advanced bioimaging, but also in intracellular drug delivery.

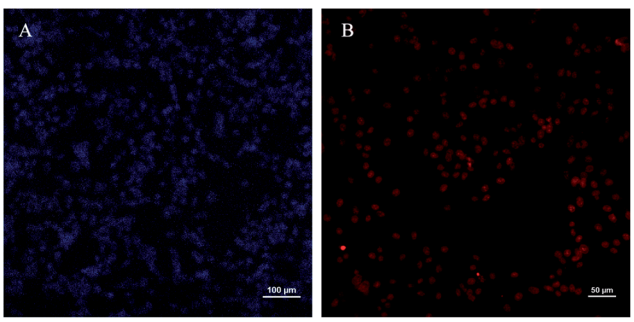

Fig. 12 CLSM images of UMUC3 cells incubated with (a) polymeric micelles and (b) DOX-loaded micelles (0.5 mg mL^{-1}) for 4 h.

4 Conclusions

Amphiphilic PCL-*b*-[PGMA-*g*-PC]-*b*-P(PEGMA) with fluorescence units was synthesized through ROP, RAFT and click chemistry. Micelles obtained from the self-assembly of amphiphilic copolymers have been used as a nano reservoir for controlled release of DOX, a model anticancer drug. These novel micelles are proved to be capable of loading high drug quantities with a reasonable loading efficiency (about 70%). The release profile of DOX from micelles in artificial urine shows a slow release in 3 days. MTT assays showed that DOX-loaded core–shell micelles exhibited high antitumor activity in UMUC3 cells, while pristine micelles were practically nontoxic up to a tested concentration of 2.0 mg mL^{-1}. These micelles with excellent biocompatibility, superior drug loading, high extracellular stability and controlled drug release are promising for the ideal drug delivery system of anticancer drugs.

Acknowledgements

The authors gratefully acknowledge the financial support of the National Natural Science Foundation of China (grant no. 51273086), the Fund for Fostering Talents from National Natural Science Foundation of China (grant no. J1103307) and Special Doctorial Program Fund from the Ministry of Education of China (grant no. 20090211110004).

References

1 L. Chang, L. Deng, W. Wang, Z. Lv, F. Hu, A. Dong and J. Zhang, *Biomacromolecules*, 2012, **13**, 3301–3310.
2 S. R. Mane, V. Rao, K. Chaterjee, H. Dinda, S. Nag, A. Kishore, J. Das Sarma and R. Shunmugam, *Macromolecules*, 2012, **45**, 8037–8042.
3 Y. Du, W. Chen, M. Zheng, F. Meng and Z. Zhong, *Biomaterials*, 2012, **33**, 7291–7299.
4 A. Li, H. P. Luehamann, G. Sun, S. Samarajeewa, J. Zou, S. Zhang, F. Zhang, M. J. Welch, Y. Liu and K. L. Wooley, *ACS Nano*, 2012, **10**, 8970–8982.
5 R. Wei, L. Cheng, M. Zheng, R. Cheng, F. Meng, C. Deng and Z. Zhong, *Biomacromolecules*, 2012, **13**, 2429–2438.
6 A. N. Lukyanov and V. P. Torchilin, *Adv. Drug Delivery Rev.*, 2004, **56**, 1273–1289.
7 R. Haag, *Angew. Chem., Int. Ed.*, 2004, **43**, 278–282.
8 G. Lapienis, *Prog. Polym. Sci.*, 2009, **34**, 852–892.
9 Z. Cheng, X. Zhu, G. D. Tu, E. T. Kang and K. G. Neoh, *Macromolecules*, 2005, **38**, 7187–7192.
10 J. C. Chen, M. Z. Liu, H. H. Gong, Y. J. Huang and C. Chen, *J. Phys. Chem. B*, 2011, **115**, 14947–14955.
11 J. L. Zhu, H. Cheng, Y. Jin, S. X. Cheng, X. Z. Zhang and R. X. Zhuo, *J. Mater. Chem.*, 2008, **18**, 4433–4439.
12 M. A. J. Gillissen, T. Terashima, E. W. Meijer, A. R. A. Palmans and I. K. Voets, *Macromolecules*, 2013, **46**, 4120–4125.
13 J. Chiefari, Y. K. B. Chong, F. Ercole, J. Krstina, J. Jeffery, T. P. T. Le, R. T. A. Mayadunne, G. F. Meijs, C. L. Moad, G. Moad, E. Rizzardo and S. H. Thang, *Macromolecules*, 1998, **31**, 5559–5562.
14 J. C. Chen, M. Z. Liu, C. M. Gao, S. Y. Lü, X. Y. Zhang and Z. Liu, *RSC Adv.*, 2013, **3**, 15085–15093.
15 J. C. Chen, M. Z. Liu, C. Chen, H. H. Gong and C. M. Gao, *ACS Appl. Mater. Interfaces*, 2011, **3**, 3215–3223.
16 A. W. York, S. E. Kirkland and C. L. McCormick, *Adv. Drug Delivery Rev.*, 2008, **60**, 1018–1036.
17 V. Coessens, T. Pintauer and K. Matyjaszewski, *Prog. Polym. Sci.*, 2001, **26**, 337–377.
18 C. W. Scales, A. J. Convertine and C. L. McCormick, *Biomacromolecules*, 2006, **7**, 1389–1392.
19 D. Bontempo, K. L. Heredia, B. A. Fish and H. D. Maynard, *J. Am. Chem. Soc.*, 2004, **126**, 15372–15373.
20 H. C. Kolb, M. G. Finn and K. B. Sharpless, *Angew. Chem., Int. Ed.*, 2001, **40**, 2004–2021.
21 C. Barner-Kowollik, F. E. Du Prez, P. Espeel, C. J. Hawker, T. Junkers, H. Schlaad and C. W. Van, *Angew. Chem., Int. Ed.*, 2011, **50**, 60–62.
22 J. C. Chen, M. Z. Liu, H. H. Gong, G. J. Cui, S. Y. Lü, C. M. Gao, F. Huang, T. Chen, X. Y. Zhang and Z. Liu, *Polym. Chem.*, 2013, **4**, 1815–1825.
23 J. Song, E. Lee and B.-K. Cho, *J. Polym. Sci., Part A: Polym. Chem.*, 2013, **51**, 446–456.
24 L. Lienafa, S. Monge and J.-J. Robin, *J. Polym. Sci., Part A: Polym. Chem.*, 2012, **50**, 3407–3414.
25 A. Gregory and M. H. Stenzel, *Prog. Polym. Sci.*, 2012, **37**, 38–105.
26 M. Kasuya, T. Taniguchi, R. Motokawa, M. Kohri, K. Kishikawa and T. Nakahira, *J. Polym. Sci., Part A: Polym. Chem.*, 2013, **51**, 4042–4051.
27 E. Chiong, K. E. Gaston and H. B. Grossman, *World J. Urol.*, 2008, **26**, 25–30.
28 D. P. Griffith, D. M. Musher and C. Itin, *Invest. Urol.*, 1976, **13**, 346–350.
29 F. Chen, Z. Cheng, J. Zhu, W. Zhang and X. Zhu, *Eur. Polym. J.*, 2008, **44**, 1789–1795.
30 T. J. Mosmann, *Immunol. Methods*, 1983, **65**, 55–63.
31 M. Li, G. L. Li, Z. Zhang, J. Li, K. G. Neoh and E. T. Kang, *Polymer*, 2010, **51**, 3377–3386.
32 F. He, T. Gädt, I. Manners and M. A. Winnik, *J. Am. Chem. Soc.*, 2011, **133**, 9095–9103.
33 Z. L. Tyrrell, Y. Shen and M. Radosz, *Prog. Polym. Sci.*, 2010, **35**, 1128–1143.
34 S. Chang, S. Chiu, C. Hsu, Y. Chang and Y. Liu, *Polymer*, 2012, **53**, 4399–4406.

